Hindawi Publishing Corporation
EURASIP Journal on Advances in Signal Processing
Volume 2010, Article ID 973286, 7 pages
doi:10.1155/2010/973286

Research Article

Time-Frequency Based Channel Estimation for High-Mobility OFDM Systems—Part II: Cooperative Relaying Case

Erol Önen, Niyazi Odabaşioğlu, and Aydın Akan (EURASIP Member)

Department of Electrical and Electronics Engineering, Istanbul University, Avcilar, 34320 Istanbul, Turkey

Correspondence should be addressed to Aydın Akan, akan@istanbul.edu.tr

Received 17 February 2010; Accepted 14 May 2010

Academic Editor: Lutfiye Durak

We consider the estimation of time-varying channels for Cooperative Orthogonal Frequency Division Multiplexing (CO-OFDM) systems. In the next generation mobile wireless communication systems, significant Doppler frequency shifts are expected the channel frequency response to vary in time. A time-invariant channel is assumed during the transmission of a symbol in the previous studies on CO-OFDM systems, which is not valid in high mobility cases. Estimation of channel parameters is required at the receiver to improve the performance of the system. We estimate the model parameters of the channel from a time-frequency representation of the received signal. We present two approaches for the CO-OFDM channel estimation problem where in the first approach, individual channels are estimated at the relay and destination whereas in the second one, the cascaded source-relay-destination channel is estimated at the destination. Simulation results show that the individual channel estimation approach has better performance in terms of MSE and BER; however it has higher computational cost compared to the cascaded approach.

1. Introduction

In wireless communication, antenna diversity is intensively used to mitigate fading effects in the recent years. This technique promises significant diversity gain. However due to the size and power limitations of some mobile terminals, antenna diversity may not be practical in some cases (e.g., Wireless Sensor Networks). Cooperative communication [1–3], also referred to as cooperative relaying, has become a popular solution for such cases since it maintains virtual antenna array without utilizing multiple antennas. Single-carrier modulation schemes are usually used in cooperative communication in the case of the flat fading channel [3]. A simple cooperative communication system with a source (S), a relay (R), and a destination (D) terminal is shown in Figure 1.

In beyond third generation and fourth generation wireless communication systems, fast moving terminals and scatterers are expected to cause the channel to become frequency selective. Orthogonal Frequency Division Multiplexing (OFDM) is a powerful solution for such channels. OFDM has a relatively longer symbol duration than single-carrier systems which makes it very immune to fast channel fading and impulsive noise. However, the overall system performance may be improved by combining the advantages of cooperative communication and OFDM systems (CO-OFDM) when the source terminal has the above-mentioned physical limitations

As in the traditional mobile OFDM systems, large fluctuations of the channel parameters are expected between and during OFDM symbols in CO-OFDM systems, especially when the terminals are mobile. To combat this problem, accurate modeling and estimation of time-varying channels are required. Early channel estimation methods for CO-OFDM assume a time-invariant model for the channel during the transmission of an OFDM symbol, which is not valid for fast-varying environments [4, 5].

A widely used channel model is a linear time-invariant impulse response where the coefficients are complex Gaussian random variables [5]. In this work we present channel estimation techniques for CO-OFDM systems over time-varying channels. We use the parametric channel model

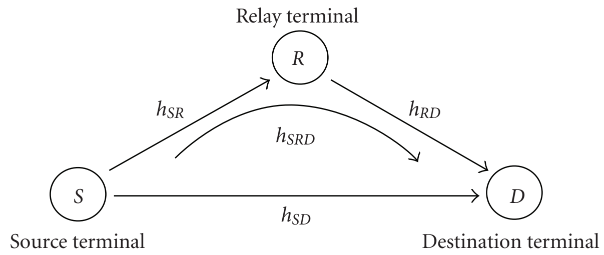

Figure 1: A simple cooperative communication system.

[6] employed in MIMO-OFDM system discussed in Part I. We consider two different scenarios similar to [7]: (i) h_{SR} is estimated at the relay, and h_{RD} is estimated at the destination individually; (ii) the cascaded channel of h_{SR} and h_{RD}, that is, the equivalent channel impulse response h_{SRD} is estimated at the destination terminal. Here h_{SR} denotes the channel response between S and R, h_{RD} denotes the channel response between R and D, and h_{SRD} is the equivalent cascaded channel response between S and D. Since no channel estimation is performed at the relay, this approach has the advantage in terms of computational requirement over the first one.

We will show here that the parameters of these individual as well as the cascaded time-varying channels can be obtained by means of time-frequency representations of the channel outputs.

The rest of the paper is organized as follows. In Section 2, we give a brief summary of the parametric channel model and CO-OFDM signal model. Section 3 presents time-frequency channel estimation for CO-OFDM systems via DET. In Section 4, we present computer simulations to illustrate the performance of proposed channel estimation in both scenarios mentioned above. Conclusions are drawn in Section 5.

2. CO-OFDM System Model

2.1. Time-Varying CO-OFDM Channel Model. In this paper, all channels are assumed multipath, fading with long-term path loss, and Doppler frequency shifts. Path loss is proportional to d^{-a} where d is the propagation distance between transmitter and receiver, and a is the path loss coefficient [8]. Let $G_{SR} = (d_{SD}/d_{SR})^a$ and $G_{RD} = (d_{SD}/d_{RD})^a$ are defined as relative gain factors of $(S \to R)$ and $(R \to D)$ links relative to $(S \to D)$ link [7, 9]. Here, d_{SD}, d_{SR}, and d_{RD} denote the distances of $(S \to D)$, $(S \to R)$, and $(R \to D)$ links, respectively.

In this study, we use the same time-varying channel model given in Section 2.2 of Part I of this series. We show here that the channel parameters between source-to-destination $(S \to D)$, source-to-relay $(S \to R)$, relay-to-destination $(R \to D)$ and the cascaded channel, and source-to-relay-to-destination $(S \to R \to D)$ may all be estimated through the spreading function of the channels. Let the channel $(S \to D)$ be given by

$$h_{SD}(m,\ell) = \sum_{i=0}^{L_{SD}-1} \lambda_i e^{j\theta_i m}\delta(\ell - D_i). \tag{1}$$

The spreading function corresponding to $h_{SD}(m,\ell)$ is obtained by taking the Fourier transform with respect to m as

$$S_{SD}(\Omega_s,\ell) = \sum_{i=0}^{L_{SD}-1} \lambda_i \delta(\Omega_s - \theta_i)\delta(k - D_i), \tag{2}$$

where L_{SD} is the number of transmission paths, θ_i represents the Doppler frequency shift, λ_i is the relative attenuation, and D_i is the delay in path i. In beyond 3G wireless mobile communication systems, Doppler frequency shifts become significant and have to be taken into account. The spreading function $S_{SD}(\Omega_s,\ell)$ displays peaks located at the time-frequency positions determined by the delays and the corresponding Doppler frequencies, with λ_i as their amplitudes. In this study, we extract the individual as well as the cascaded channel information from the spreading function of the received signals at the relay and at the destination.

The cascaded source-to-relay-to-destination $(S \to R \to D)$ channel may be represented in terms of the individual channels as follows. Let the $(S \to R)$ and the $(R \to D)$ channels be given by

$$\begin{aligned} h_{SR}(m,\ell) &= \sum_{i=0}^{L_{SR}-1} \alpha_i e^{j\psi_i m}\delta(\ell - N_i), \\ h_{RD}(m,\ell) &= \sum_{i=0}^{L_{RD}-1} \beta_i e^{j\varphi_i m}\delta(\ell - M_i). \end{aligned} \tag{3}$$

The equivalent impulse response of the cascaded $(S \to R \to D)$ channel may be obtained as follows:

$$\begin{aligned} h_{SRD}(m,\ell) &= h_{SR}(m,\ell) \star h_{RD}(m,\ell) \\ &= \sum_r h_{SR}(m,r)h_{RD}(m,\ell - r) \\ &= \sum_r \sum_{i=0}^{L_{SR}-1} \alpha_i e^{j\psi_i m}\delta(r - N_i) \\ &\quad \times \sum_{q=0}^{L_{RD}-1} \beta_q e^{j\varphi_q m}\delta\left(\ell - r - M_q\right) \\ &= \sum_{i=0}^{L_{SR}-1} \alpha_i e^{j\psi_i m} \sum_{q=0}^{L_{RD}-1} \beta_q e^{j\varphi_q m}\delta\left(\ell - N_i - M_q\right) \\ &= \sum_{i=0}^{L_{SR}-1}\sum_{q=0}^{L_{RD}-1} \alpha_i\beta_q e^{j(\psi_i+\varphi_q)m}\delta\left(\ell - N_i - M_q\right), \end{aligned} \tag{4}$$

where $\star$ stands for convolution. After defining the parameters $L_{SRD} = L_{SR}L_{RD}$, $z = iL_{RD} + q$, $\gamma_z = \alpha_i + \beta_q$, $\xi_z = \psi_i + \varphi_q$, and $Q_z = N_i + M_q$, we obtain the impulse response of the cascaded ($S \rightarrow R \rightarrow D$) channel as

$$h_{SRD}(m,\ell) = \sum_{z=0}^{L_{SRD}-1} \gamma_z e^{j\xi_z}\delta(\ell - Q_z). \quad (5)$$

In our second approach, instead of estimating the individual channel parameters, we obtain the equivalent γ_z, ξ_z, and Q_z parameters.

2.2. CO-OFDM Signal Model. We consider an Amplify-and-Forward (AF) cooperative transmission model where a source sends information to a destination with the assistance of a relay [3, 10]. In this model, all of the terminals are equipped with only one transmit and one receive antenna. To manage cooperative transmission, we consider a special protocol which is originally proposed in [10] and named "Protocol II". According to this protocol, total transmission is divided in two phases. In Phase I, source sends OFDM signal to both relay and destination terminals. Relay terminal amplifies the received signal in the same phase. In Phase II, relay terminal transmits the amplified signal to the destination terminal.

The OFDM symbol transmitted from the source at Phase I is given by

$$s(m) = \frac{1}{\sqrt{K}}\sum_{k=0}^{K-1} X_k e^{j\omega_k m}, \quad (6)$$

where $m = -L_{CP}, -L_{CP}+1, \ldots, 0, \ldots, K-1$, L_{CP} is the length of the cyclic prefix, and $N = K + L_{CP}$ is the total length of one OFDM symbol. The received signals at relay and destination suffer from time and frequency dispersion of the channels, that is, multipath propagation, fading and Doppler frequency shifts. Thus, the received signals at the relay and destination in Phase I are

$$\begin{aligned} r_R(m) &= \sqrt{G_{SR}E}\sum_{\ell=0}^{L_{SR}-1} h_{SR}(m,\ell)s(m-\ell) + n_R(m) \\ &= \sqrt{G_{SR}E}\frac{1}{\sqrt{K}}\sum_{k=0}^{K-1} X_k \sum_{i=0}^{L_{SR}-1}\alpha_i e^{j\psi_i m}e^{j\omega_k(m-N_i)} + n_R(m), \\ r_{D1}(m) &= \sqrt{G_{SD}E}\sum_{\ell=0}^{L_{SD}-1} h_{SD}(m,\ell)s(m-\ell) + n_{D1}(m) \\ &= \sqrt{G_{SD}E}\frac{1}{\sqrt{K}}\sum_{k=0}^{K-1} X_k \sum_{i=0}^{L_{SD}-1}\alpha_i e^{j\psi_i m}e^{j\omega_k(m-N_i)} + n_{D1}(m), \end{aligned} \quad (7)$$

where $n_R(m)$ and $n_{D1}(m)$ represent the additive white Gaussian channel noise at ($S \rightarrow R$) and ($R \rightarrow D$) channels, respectively. Here E represents the transmitted OFDM symbol energy. The signal $r_R(m)$ is amplified by a factor $1/\sqrt{E[\|r_R\|^2]}$ at the relay and then transmitted to the destination in Phase II. The signal at the output of $R \rightarrow D$ channel, received by the destination terminal, is

$$r_{D2}(m) = \sqrt{G_{RD}E}\sum_{\ell=0}^{L_{RD}-1} h_{RD}(m,\ell)\frac{r_R(m-\ell)}{\sqrt{E\left[\|r_R\|^2\right]}} + n_{D2}(m). \quad (8)$$

Now, using the cascaded equivalent of $h_{SR}(m,\ell)$ and $h_{RD}(m,\ell)$ from (5), we get

$$\begin{aligned} r_{D2}(m) &= \sqrt{\frac{G_{SR}G_{RD}E^2}{E[\|r_R\|^2]}}\left(\sum_{z=0}^{L_{SRD}-1} h_{SRD}(m,z)s(m-\ell) + n'_R(m)\right) \\ &\quad + n_{D2}(m) \\ &= \sqrt{\frac{G_{SR}G_{RD}E^2}{E[\|r_R\|^2]}} \\ &\quad \times\left(\frac{1}{\sqrt{K}}\sum_{z=0}^{L_{SRD}-1}\sum_{k=0}^{K-1}\gamma_z e^{j\xi_z m}e^{j\omega_k(m-Q_z)} + n'_R(m)\right) \\ &\quad + n_{D2}(m), \end{aligned} \quad (9)$$

where $n'_R(m)$ is the response of the ($R \rightarrow D$) channel to the $n_R(m)$ noise

$$n'_R(m) = \sum_{\ell=0}^{L_{RD}-1} h_{RD}(m,\ell)n_R(m-\ell). \quad (10)$$

The receiver at the destination terminal discards the cyclic prefix and demodulates the received signals $r_{D1}(m)$ and $r_{D2}(m)$ using a K-point DFTs. For example the demodulated signal corresponding to $r_{D1}(m)$ is

$$\begin{aligned} R_{D1_k} &= \frac{1}{\sqrt{K}}\sum_{m=0}^{K-1} r_{D1}(m)e^{-j\omega_k m} \\ &= \frac{1}{K}\left(\sum_{m=0}^{K-1}\sum_{s=0}^{K-1} X_s \sum_{i=0}^{L_{SD}-1}\lambda_i e^{j\theta_i m}e^{j\omega_s(m-D_i)}\right)e^{-j\omega_k m} + \mathcal{N}_{D1_k} \\ &= \frac{1}{K}\sum_{s=0}^{K-1} X_s \sum_{i=0}^{L_{SD}-1}\lambda_i e^{-j\omega_s D_i}\sum_{m=0}^{K-1} e^{j\theta_i m}e^{j(\omega_s-\omega_k)m} + \mathcal{N}_{D1_k}. \end{aligned} \quad (11)$$

If the Doppler shifts in all $S \rightarrow D$ channel paths are negligible, $\theta_i \approx 0$, for all i, then the channel is almost time-invariant within one OFDM symbol, and

$$\begin{aligned} R_{D1_k} &= X_k \sum_{i=0}^{L_{SD}-1}\lambda_i e^{-j\omega_k D_i} + \mathcal{N}_{D1_k} \\ &= X_k H_k + \mathcal{N}_{D1_k}, \end{aligned} \quad (12)$$

where H_{SDk} is the frequency response of the *almost time-invariant* channel and $\mathcal{N}_{D1_k}$ is the DFT of the $r_{D1}(m)$. By estimating the channel frequency response coefficients H_{SDk}, data symbols, X_k, can be recovered according to (12). Estimation of the channel coefficients is usually achieved by using training symbols P_k, called pilots inserted between data symbols. Then the transfer function is interpolated from the responses to P_k by using different filtering techniques. This is called Pilot Symbol Assisted (PSA) channel estimation [11].

However, in beyond 3G communication systems, fast moving terminals and scatterers are expected in the environment, causing the Doppler frequency shifts to become significant which makes the above assumption invalid. In this paper, we consider a completely time-varying model for the CO-OFDM channels where the parameters may change during one transmit symbol [12], based on the time-frequency approach.

3. Time-Varying Channel Estimation for CO-OFDM Systems

In this section we consider the estimation procedure of time-varying CO-OFDM channels $(S \to R)$, $(R \to D)$ as well as the cascaded $(S \to R \to D)$ channels. We approach the channel estimation problem from a time-frequency point of view and employ the channel estimation technique proposed in Part I of this series. Details on the Discrete Evolutionary Transform (DET) that we use here as a time-frequency representation of time-varying CO-OFDM channels may be found in Section 3 of Part I.

The time-varying frequency response or equivalently the spreading function of the individual as well as the cascaded channels may be calculated by means of the DET of the received signal.

We consider two channel estimation approaches for the CO-OFDM system illustrated in Figure 1.

3.1. Individual Channel Estimation Approach. The $(S \to R)$ channel is estimated at the relay terminal, then the transmitted signal is amplified, and new pilot symbols are inserted for the estimation of $(R \to D)$ channel. The pilot symbols that are inserted at the source are effected by the multipath fading nature of the $(S \to R)$ channel, as such may not be used for the estimation of $(R \to D)$ channel. Therefore, we need to insert fresh pilot symbols and extend the length of the OFDM symbol at the relay. The estimated $(S \to R)$ channel information is quantized and transmitted to the destination together with the data symbols. Then at the destination terminal, the $(R \to D)$ channel is estimated and used for the detection. Parameters of both $h_{SR}(m,\ell)$ and $h_{RD}(m,\ell)$ channel impulse responses are estimated according to the procedure explained in Section 3 of Part I.

3.2. Cascaded Channel Estimation Approach. The relay terminal does not perform any channel estimation. The cascaded $(S \to R \to D)$ channel is estimated at the destination terminal.

The received signal $r_{D2}(m)$ can be given in matrix form as

$$\mathbf{r} = \mathbf{A}\mathbf{x}, \tag{13}$$

where

$$\begin{gathered}\mathbf{r} = [r_{D2}(0), r_{D2}(1), \ldots, r_{D2}(K-1)]^T, \\ \mathbf{x} = [X_0, X_1, \ldots, X_{K-1}]^T, \\ \mathbf{A} = [a_{m,k}]_{K\times K}, \qquad a_{m,k} = \frac{H_{SRD}(m,\omega_k)e^{j\omega_k m}}{\sqrt{K}}.\end{gathered} \tag{14}$$

We ignore the additive noise in the sequel to simplify the equations. If the time-varying frequency response of the channel $H_{SRD}(m,\omega_k)$ is known, then X_k may be estimated by

$$\hat{\mathbf{x}} = \mathbf{A}^{-1}\mathbf{r}. \tag{15}$$

Calculating the DET of $r_{D2}(m)$, we get

$$\begin{aligned} r_{D2}(m) &= \sum_{k=0}^{K-1} R_{D2}(m,\omega_k)e^{j\omega_k m}, \\ &= \frac{1}{\sqrt{K}} \sum_{k=0}^{K-1} H_{SRD}(m,\omega_k) X_k e^{j\omega_k m}, \end{aligned} \tag{16}$$

where $R_{D2}(m,\omega_k)$ is the time-varying kernel of the DET transform. Comparing the above representations of $r_{D2}(m)$, we require that the kernel is

$$R_{D2}(m,\omega_k) = \frac{1}{\sqrt{K}} \sum_{i=0}^{L_{SRD}-1} \gamma_i e^{j\xi_i m} e^{-j\omega_k Q_i} X_k. \tag{17}$$

Finally, the time-varying channel frequency response for the nth OFDM symbol can be obtained as

$$H_{SRD}(m,\omega_k) = \frac{\sqrt{K} R_{D2}(m,\omega_k)}{X_k}. \tag{18}$$

Calculation of $R_{D2}(m,\omega_k)$ in such a way that it satisfies (17) is explained in Section 3 of Part I by using windows that are adapted to the Doppler frequencies.

According to the above equation, we need the input pilot symbols P_k to estimate the channel frequency response. Here we consider simple, uniform pilot patterns; however improved patterns may be employed as well [11].

Equation (18) can be given in matrix form as

$$\mathbf{H} = \sqrt{K}\mathbf{R}\mathbf{X}^{-1}, \tag{19}$$

where

$$\begin{gathered}\mathbf{H} \triangleq [h_{m,k}]_{K\times K}, \qquad h_{m,k} = H_{SRD}(m,\omega_k), \\ \mathbf{R} \triangleq [r_{m,k}]_{K\times K}, \qquad r_{m,k} = R_{D2}(m,\omega_k), \\ \mathbf{X} \triangleq \mathbf{I}\mathbf{x},\end{gathered} \tag{20}$$

where $\mathbf{I}$ denotes a $K \times K$ identity matrix. The above relation is also valid at the preassigned pilot positions $k = k'$

$$H'_{SRD}\left(m, \omega_p\right) = H_{SRD}(m, \omega_{k'}) = \frac{\sqrt{K} R_{D2}(m, \omega_{k'})}{X_{k'}}, \quad (21)$$

where $p = 1, 2 \ldots, P$ and $H'_{SRD}(m, \omega_p)$ is a decimated version of the $H_{SRD}(m, \omega_k)$. Note that P is again the number of pilots, and $d = K/P$ is the distance between adjacent pilots. Taking the inverse DFT of $H'_{SRD}(m, \omega_p)$ with respect to ω_p and DFT with respect to m, we obtain the subsampled spreading function $S'_{SRD}(\Omega_s, \ell)$

$$S'_{SRD}(\Omega_s, \ell) = \frac{1}{d} \sum_{i=0}^{L_{SRD}-1} \gamma_i \delta(\Omega_s - \xi_i) \delta\left(\frac{\ell - Q_i}{d}\right). \quad (22)$$

Note that, the evolutionary kernel $R_{D2}(m, \omega_k)$ can be calculated directly from $r_{D2}(m)$, and all unknown channel parameters can be estimated according to (21) and (22) for a time-varying model that does not require any stationarity assumption. Estimated channel parameters are used for the detection at the destination terminal according to the channel equalization algorithm presented in Section 3.2 of Part I.

In the following, we demonstrate the time-frequency channel estimation as well as the detection performance of our approach by means of examples.

4. Experimental Results

In our simulations, a CO-OFDM system scenario with a source, a relay, and a destination terminal is considered with the following parameters: the distances d_{SR} and d_{RD} are chosen such that the relative gain ratio G_{SR}/G_{RD} takes the values $\{-40, 0, 40\}$ dB, where the path loss coefficient is assumed to be $a = 2$ [7]. The angle between $S \rightarrow R$ and $R \rightarrow D$ propagation paths is taken as $\theta = 2\pi/3$. The performance of both individual and cascaded channel estimation approaches is investigated by means of the mean square error (MSE) and the bit error rate (BER) according to varying signal-to-noise ratios. QPSK-coded data symbols X_k are modulated onto $K = 128$ subcarriers to generate one OFDM symbol. 16 equally spaced pilot symbols are inserted into OFDM symbols. The $S \rightarrow R$, $R \rightarrow D$, and $S \rightarrow D$ channels are simulated randomly. For each of these channels, the maximum number of paths is set to $L = 5$ where the delays and the attenuations on each path are chosen as independent, normal distributed random variables. Normalized Doppler frequency on each path is fixed to $f_D = 0.2$ [12].

The channel output is corrupted by zero-mean AWGN whose SNR is changed between 0 and 35 dB.

(1) Individual Channel Estimation Results. The $S \rightarrow R$ and $R \rightarrow D$ channels are estimated at the corresponding terminals and are available at the destination. Moreover, the $S \rightarrow D$ channel is estimated at the destination by using the signal $r_{D1}(m)$. Then data symbols are detected from the received signals $r_{D1}(m)$ and $r_{D2}(m)$ by using this channel information. Figure 2(a) shows the total MSE of the channel estimations $S \rightarrow R$ and $R \rightarrow D$ for $G_{SR}/G_{RD} = \{-40, 0, 40\}$ in dB. We see that we obtain the best channel estimation for 0 dB which corresponds to equal distance between $S \rightarrow R$ and $R \rightarrow D$. We give the BER performances at different channel noise levels for $G_{SR}/G_{RD} = \{-40, 0, 40\}$ dB in Figure 2(b). We also compare and present our results with the performance of the perfect channel state information (CSI) in the same figure. Similar to the MSE, we have the closest BER performance to the perfect CSI for the case of $G_{SR}/G_{RD} = 0$ dB. We observe from this figure that, the "individual approach for 0 dB" has about 5 dB SNR gain over the "individual 40 dB" at BER $= 10^{-4}$.

(2) Cascaded Channel Estimation Results: The combined $S \rightarrow R \rightarrow D$ channel is estimated at the destination terminal from $r_{D2}(m)$. The $S \rightarrow D$ channel is estimated at the destination by using the signal $r_{D1}(m)$. Data symbols are detected from $r_{D1}(m)$ and $r_{D2}(m)$ by using estimated channel parameters. Figure 3(a)

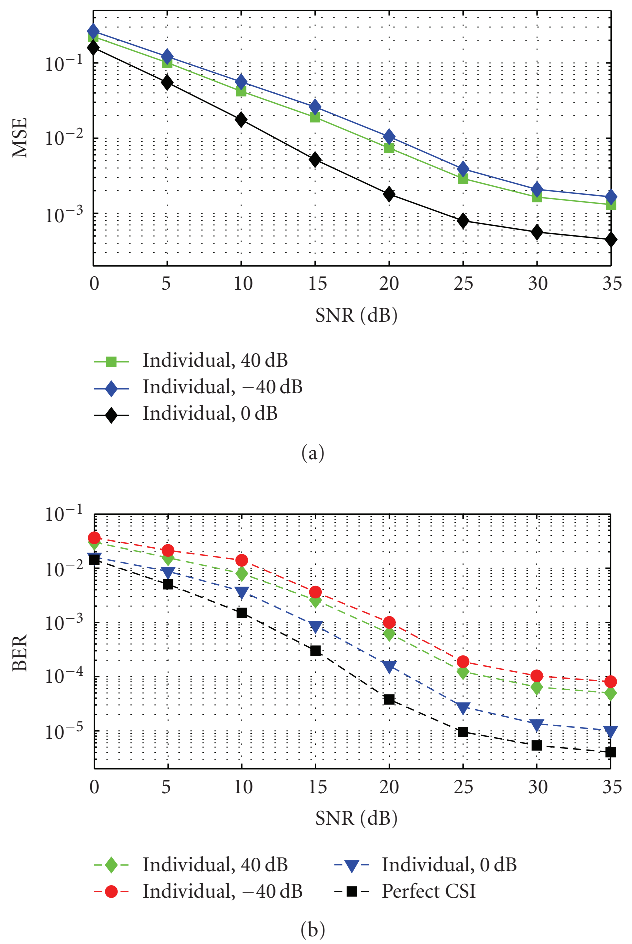

Figure 2: Performance of the individual channel estimation approach. (a) MSE versus SNR, (b) BER performance versus SNR.

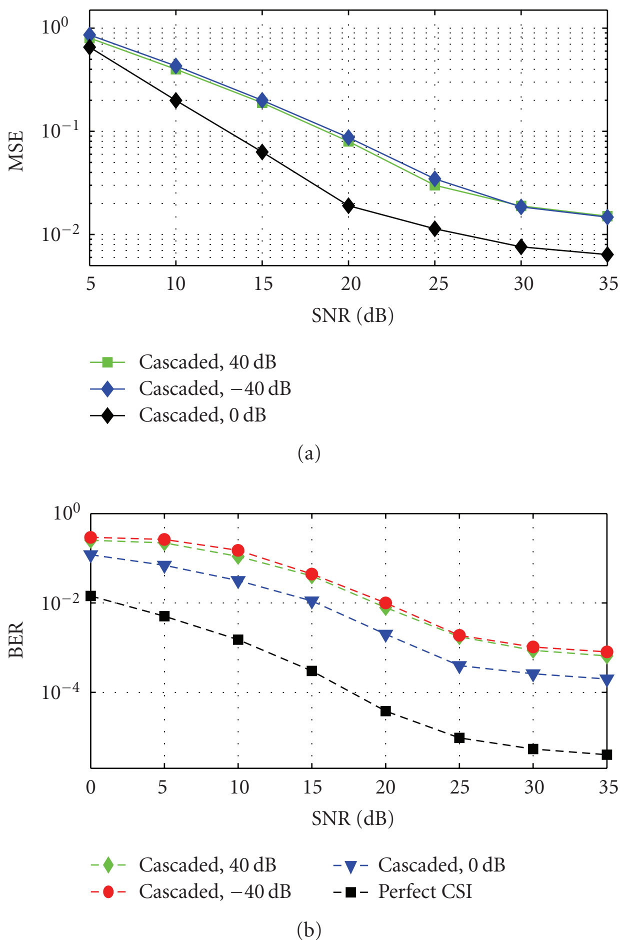

Figure 3: Performance of the cascaded channel estimation approach. (a) Change in the MSE by SNR, (b) BER versus SNR.

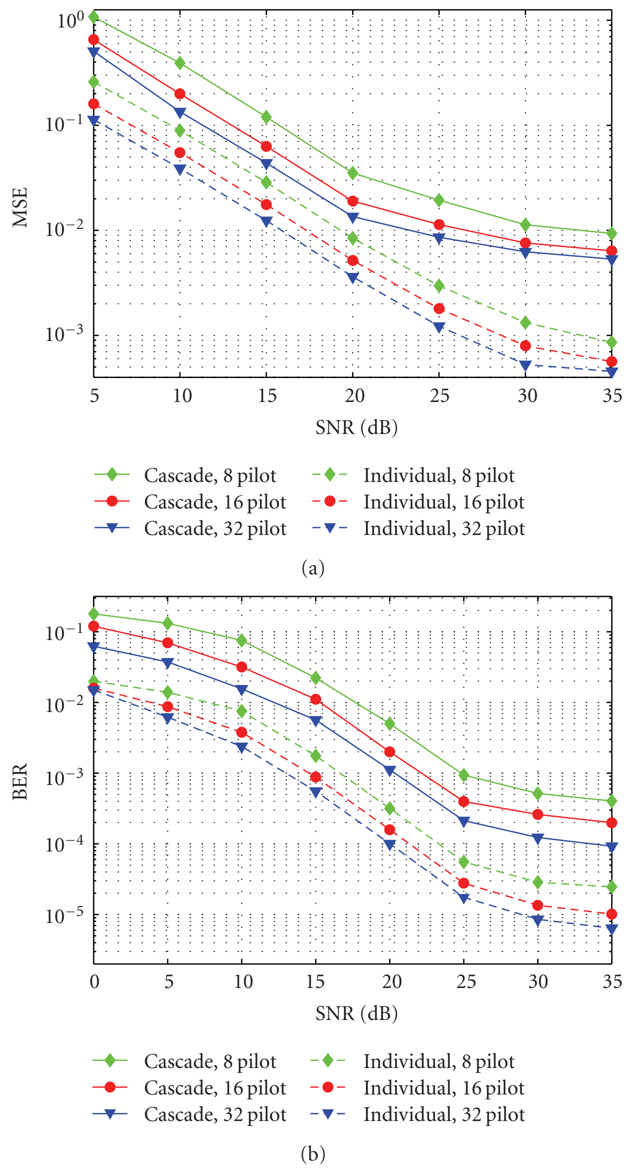

Figure 4: Effect of the number of pilots in both approaches. (a) Change of MSE by SNR, (b) change of BER by SNR.

shows the MSE of the cascaded $S \rightarrow R \rightarrow D$ channel estimation for $G_{SR}/G_{RD} = \{-40, 0, 40\}$ dB. Note that we obtain almost the same estimation performance for -40 and 40 dB and obtain better results for $G_{SR}/G_{RD} = 0$ dB as in the individual channel estimation case. We show the BER performance for $G_{SR}/G_{RD} = \{-40, 0, 40\}$ dB, as well as for the perfect CSI case in Figure 3(b). The noise floors in the figures are due to the fact that we do not consider advanced detection techniques for the receiver in our studies. Our main concern is the estimation of the time-varying channel. By using more advanced detection methods, error floors shown in our figures may be reduced.

Notice that the individual channel estimation approach outperforms the cascaded approach in terms of both MSE and BER as expected, at the expense of twice the computational complexity. This comes from the fact that relay terminal estimates the channel and transmits to the destination with an increased symbol duration due to the insertion of new pilot symbols. In approach two, the relay does not perform any channel estimation; hence the computational burden is reduced. However, the estimated combined channel parameters are not as reliable as in the first approach.

We have also investigated the effect of the number of pilots to the channel estimation performance in both approaches. We show the BER and MSE plots in Figures 4(a) and 4(b), respectively, for $P = \{8, 16, 32\}$. Notice that increasing the number of pilots improves the BER performance in both approaches especially the cascaded approach.

The effect of the number of channel paths on the BER is illustrated by a simulation where the number of pilots is taken as $P = \{8, 16\}$ and the SNR = 15 dB. The number of

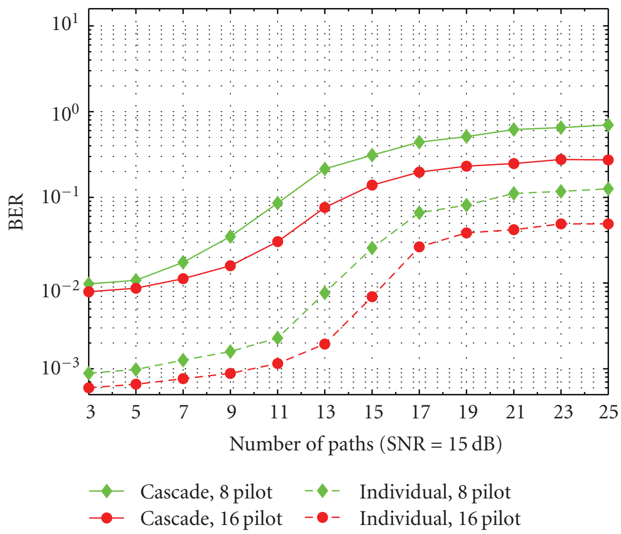

Figure 5: BER performance change by the number of channel paths for 8 and 16 pilots, and 15 dB SNR.

paths is changed between 3 and 25, and the BER is presented in Figure 5. Note that both approaches equally suffer from increasing the number of paths.

5. Conclusions

In this paper, we present a time-varying channel estimation technique for CO-OFDM systems. We propose two approaches where in the first one, individual channels are estimated at the relay and destination whereas in the second approach, the cascaded source-relay-destination channel is estimated at the destination. We assume that the communication channels are multipath and affected by considerable Doppler frequencies. Simulation results show that the individual channel estimation approach gives better performance than the cascaded approach in terms of both estimation error and the bit error rate. However, in the cascaded channel estimation case, the computational cost is reduced significantly at the expense of decreased performance. We observe that the best performance is achieved when the distances of source-to-relay and relay-to-destination is equal, for both approaches.

Acknowledgment

This work was supported by The Research Fund of The University of Istanbul, project nos. 6904, 2875, and 6687.

References

[1] A. Sendonaris, E. Erkip, and B. Aazhang, "User cooperation diversity—part I: system description," *IEEE Transactions on Communications*, vol. 51, no. 11, pp. 1927–1938, 2003.

[2] A. Sendonaris, E. Erkip, and B. Aazhang, "User cooperation diversity—part II: implementation aspects and performance analysis," *IEEE Transactions on Communications*, vol. 51, no. 11, pp. 1939–1948, 2003.

[3] J. N. Laneman, D. N. C. Tse, and G. W. Wornell, "Cooperative diversity in wireless networks: efficient protocols and outage behavior," *IEEE Transactions on Information Theory*, vol. 50, no. 12, pp. 3062–3080, 2004.

[4] H. Doğan, "Maximum a posteriori channel estimation for cooperative diversity orthogonal frequency-division multiplexing systems in amplify-and-forward mode," *IET Communications*, vol. 3, no. 4, pp. 501–511, 2009.

[5] Z. Zhang, W. Zhang, and C. Tellambura, "Cooperative OFDM channel estimation in the presence of frequency offsets," *IEEE Transactions on Vehicular Technology*, vol. 58, no. 7, pp. 3447–3459, 2009.

[6] P. A. Bello, "Characterization of randomly time-variant linear channels," *IEEE Transactions on Communication Systems*, vol. 11, pp. 360–393, 1963.

[7] O. Amin, B. Gedik, and M. Uysal, "Channel estimation for amplify-and-forward relaying: Cascaded against disintegrated estimators," *IET Communications*, vol. 4, no. 10, pp. 1207–1216, 2010.

[8] J. W. Mark and W. Zhuang, *Wireless Communication and Networking*, Prentice Hall, Upper Saddle River, NJ, USA, 2003.

[9] H. Ochiai, P. Mitran, and V. Tarokh, "Variable-rate two-phase collaborative communication protocols for wireless networks," *IEEE Transactions on Information Theory*, vol. 52, no. 9, pp. 4299–4313, 2006.

[10] R. U. Nabar, H. Bölcskei, and F. W. Kneubühler, "Fading relay channels: performance limits and space-time signal design," *IEEE Journal on Selected Areas in Communications*, vol. 22, no. 6, pp. 1099–1109, 2004.

[11] S. G. Kang, Y. M. Ha, and E. K. Joo, "A comparative investigation on channel estimation algorithms for OFDM in mobile communications," *IEEE Transactions on Broadcasting*, vol. 49, no. 2, pp. 142–149, 2003.

[12] Z. Tang, R. C. Cannizzaro, G. Leus, and P. Banelli, "Pilot-assisted time-varying channel estimation for OFDM systems," *IEEE Transactions on Signal Processing*, vol. 55, no. 5, pp. 2226–2238, 2007.